JST: Smart Systems and Devices
Volume 35, Issue 1, January 2025, 065-073

Simulation Approach to Investigate the Influence of the Steering Wheel Angle and Vehicle Speed on the Rollover of a 4-Axle Truck Vehicle during Turning Maneuvers

Ta Tuan Hung[1], Duong Ngoc Khanh[2*]
[1]University of Transport Technology, Ha Noi, Vietnam
[2]Hanoi University of Science and Technology, Ha Noi, Vietnam
[*]Corresponding author email: khanh.duongngoc@hust.edu.vn

Abstract

The article aims to investigate the influence of vehicle speed and steering wheel angle on the rollover condition of a 4-axle truck vehicle. A 30-degree-of-freedom (DOF) dynamic model of a 4-axle truck is established using the Multibody System Method and the Newton-Euler equation system. The vehicle body is described with 6 DOFs. Additionally, 2 DOFs are used to describe the roll motion of the front and rear masses of the vehicle body, taking into account the influence of the torsional stiffness of the vehicle frame on vehicle dynamics. The Burckhardt tire model calculates the interaction forces between tires and the road, using experimental coefficients corresponding to the road with a maximum adhesion coefficient of 0.8. The simulation uses MATLAB-Simulink, with a 5 to 65 km/h speed range and a steering wheel rotation angle ranging from 25 to 300 degrees. The results have determined the vehicle rollover conditions based on the signs of the load transfer ratio of the axle and the entire vehicle. Together with the results of lateral acceleration, yaw rate, and roll angle of the vehicle. This result can be used to propose dynamic thresholds for designing early warning systems and anti-rollover control systems for multi-axle truck vehicles.

Keywords: Full dynamics model, Burckhardt tire model, Multibody System Method, 4-axle truck vehicle.

1. Introduction

In recent years, there has been a significant increase in the number of accidents involving truck vehicles, particularly multi-axle vehicles and articulated vehicles. These vehicles are large in size and weight, making them prone to rollovers during turns or lane changes, as well as collisions with obstacles. This instability has been a major contributing factor to many truck accidents. According to the Insurance Institute for Highway Safety, there were 4,714 deaths in the US in 2021 due to collisions involving large trucks. Statistics also show that 52% of these fatal accidents were caused by large trucks [1]. In Korea, truck accidents accounted for approximately 13% of all accidents and 24% of total deaths in 2019 [2].

Many truck accidents occur due to unstable motion, particularly lateral instability such as rollover, side slipping [3, 4]. Rollover, on the other hand, is caused by a large inertial force that creates a moment strong enough to be a greater anti-rollover moment, causing the rollover of the vehicle. This state can occur during turning maneuvers on roads with high adhesion coefficients, or even when colliding with other objects on roads with low adhesion coefficients [5, 6]. The structure of multiple steering axles and the kinematic alignment of the steering axle ensure the vehicle is more stable when turning [7].

In recent years, there have been numerous studies conducted on the lateral stability of truck vehicles. These studies have yielded results that evaluate the potential for rollover and side sliding in various motion conditions, such as braking and turning, particularly at high speeds. For example, Lundahl [8] analyzed and evaluated the side rollover criteria for truck vehicles with load transfer ratio (*LTR*) and proposed a maximum lateral acceleration threshold of 0.55gm/s^2 when Quarter-Circle Maneuver at a speed of 45km/h. Researchers have developed dynamic models for trucks in different planes (yaw and roll) or in space (full dynamics model) [9]. For vehicles with multiple steering axles or suspension system links, the connections are described using several degrees of freedom to accurately simulate the interactions between the axles [10]. The evaluation of potential instability depends on the results calculated from the types of established models [5].

ISSN: 2734-9373
https://doi.org/10.51316/jst.179.ssad.2025.35.1.8
Received: 05 Jun 2024; revised: 12 Jul 2024;
accepted: 12 Jul 2024

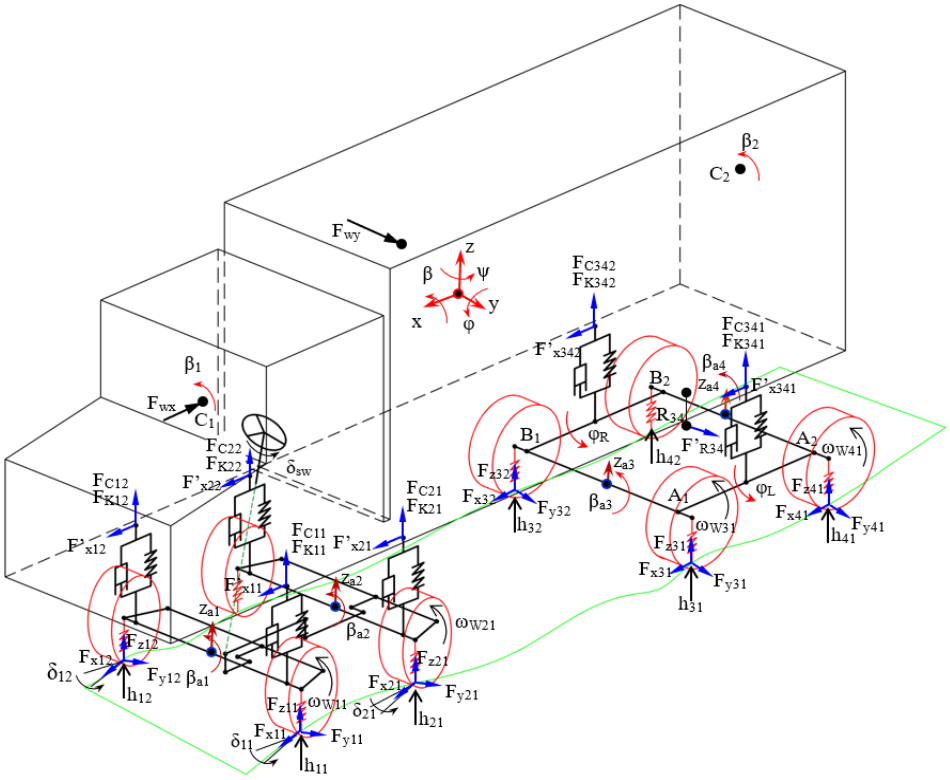

Fig. 1. Schematic of the dynamics model of a 4-axle truck vehicle

In this article, a 30-degree-of-freedom (DOF) full dynamics model is established using the Multibody System Method, and a detailed nonlinear tire model is presented. The model is simulated using MATLAB Simulink software to evaluate the lateral stability of a 4-axle truck vehicle during turning maneuvers on a wet asphalt road. The results of this study can serve as a basis for designing control systems to improve the lateral stability of 4-axle truck vehicles.

2. Full Dynamics Model of 4-Axle Truck Vehicle

Some assumptions are proposed as follows: (1) the wheels are elastic when moving on a flat road; (2) the elastic influence of the steering system is ignored; (3) the points of applied forces from the suspension system correspond to the midpoint of the leaf springs; (4) the lateral linkage forces of the vehicle body and the vehicle axles are referred to the corresponding roll centers at the axle.

The Multibody System Method [11] and the Newton-Euler equation system [5] are utilized to formulate a set of mathematical equations that describe the motion of a 4-axle truck vehicle. The vehicle body is characterized by 6 DOFs: longitudinal translation, lateral translation, vertical translation, roll rotation, pitch rotation, and yaw rotation. To accurately simulate the impact of frame torsional stiffness on the vehicle's dynamics, two roll motions of the front and rear mass of the vehicle body are incorporated, each with 2 DOFs. The four axles are represented by 3 DOFs: lateral translation, vertical translation, and roll rotation for each axle. Additionally, the 8 wheels are described as having a DOF for wheel rotation. The reference systems are conventionally defined as follows.

The fixed coordinate system *OXYZ* is located at the ground; The body coordinate system *Cxyz* is located at the Center of Gravity of the vehicle body; The axle coordinate systems $A_i x_{Ai} y_{Ai} z_{Ai}$ (i=1÷4) are located at the CoG of the axles, respectively; The wheel coordinate systems $W_{ij} x_{Wij} y_{Wij} z_{Wij}$ (i=1÷4;j=1÷2) is located at the center of wheel.

2.1. Motion Equation System of the Vehicle Body

The Newton-Euler equation system for the vehicle body is written as follows:

$$\begin{cases} m(\dot{v}_x - v_y\omega_z + v_z\omega_y) = F_X \\ m(\dot{v}_y - v_z\omega_x + v_x\omega_z) = F_Y \\ m(\dot{v}_z - v_x\omega_y + v_y\omega_x) = F_Z \\ I_x\dot{\omega}_x + (I_z - I_y)\omega_z\omega_y = M_X \\ I_y\dot{\omega}_y + (I_x - I_z)\omega_x\omega_z = M_Y \\ I_z\dot{\omega}_z + (I_y - I_x)\omega_y\omega_x = M_Z \end{cases} \quad (1)$$

where: m is the mass of the vehicle body; I_x, I_y, and I_z are the moment of inertia of the vehicle body along *Cx*, *Cy*, and *Cz*, respectively; v_x, v_y, and v_z are translational velocities; ω_x, ω_y, ω_z are the rotational velocities.

F_X refers to the combined external forces acting in the direction of Cx. These forces include those transmitted from the axles to the suspended mass (F'_{xij}), the aerodynamic drag force (F_{wx}), and the dynamic force caused by the weight of the suspended vehicle body in the Cx direction. This can be expressed as follows.

$$F_X = F'_{x11} + F'_{x12} + F'_{x21} + F'_{x22} + F'_{x341} + F'_{x342} + mg\sin\varphi - F_{wx} \quad (2)$$

F_Y represents the combined external forces acting in the direction of Cy, which includes the lateral forces at the roll center (F'_{R1}, F'_{R2}, F'_{R34}), the lateral aerodynamic drag force (F_{wy}), and the dynamic force caused by the weight of the suspended vehicle body. This can be expressed as follows:

$$F_Y = F'_{R1} + F'_{R2} + F'_{R34} - mg\cos\varphi\sin\beta + F_{wy} \quad (3)$$

F_Z is the total external force acting on the Cz direction, determined by the leaf spring forces F_{Cij}, the damping force F_{Kij}, and the gravity force of the suspended vehicle body, which can be written as follows:

$$F_Z = F_{C11} + F_{C12} + F_{K11} + F_{K12} + F_{C11} + F_{C22} + F_{K21} + F_{K22} + F_{C341} + F_{C342} + F_{K341} + F_{K342} + mg(1 - \cos\varphi\cos\beta) \quad (4)$$

M_X is the sum of external force moments along the Cx axis, written as follows:

$$\begin{aligned} M_X = {} & w_1(F_{C11} + F_{K11} - F_{C12} - F_{K12}) + \\ & w_2(F_{C21} + F_{K21} - F_{C22} - F_{K22}) + \\ & w_{34}(F_{C341} + F_{K341} - F_{C342} - F_{K342}) + \\ & (h - h_{R1})F'_{R1} + (h - h_{R2})F'_{R2} + (h_1 - h_{R34})F'_{R34} - \\ & (h_w - h)F_{wy} - (M_{T1} + M_{T2} + M_{T3} + M_{T4}) \end{aligned} \quad (5)$$

M_Y is the total external force moment along the Cy axis written as follows:

$$\begin{aligned} M_Y = {} & -l_1(F_{C11} + F_{K11} + F_{C12} + F_{K12}) - l_2(F_{C21} + F_{K21} + F_{C22} + F_{K22}) \\ & + (l_3 + \frac{a}{2})(F_{C341} + F_{K341} + F_{C342} + F_{K342}) \\ & - (h - r_1)(F'_{x11} + F'_{x12} + F'_{x21} + F'_{x22} + F'_{x341} + F'_{x342}) \\ & - (M_{11} + M_{12} + M_{21} + M_{22} + M_{341} + M_{342}) - (h_w - h)F_{wx} \end{aligned} \quad (6)$$

M_Z is the total external force moment along the Cz axis, written as follows:

$$\begin{aligned} M_Z = {} & w_1(F'_{x12} - F'_{x11}) + w_2(F'_{x22} - F'_{x21}) + \\ & w_{34}(F'_{x342} - F'_{x341}) + l_1F'_{R1} + l_2F'_{R2} - (\frac{l_3 + l_4}{2})F'_{R34} \end{aligned} \quad (7)$$

To consider the torsional of the vehicle frame, the two equations determining the front mass and rear mass roll rotation of the vehicle body are determined by the following two equations as:

$$\begin{cases} I_{x1}\ddot{\beta}_1 = w_1(F_{C11} + F_{K11} - F_{C12} - F_{K12}) + w_2(F_{C21} + F_{K21} - F_{C22} - F_{K22}) \\ \qquad - \mathrm{M}_{T1} - M_{T2} - M_{kx} \\ I_{x2}\ddot{\beta}_2 = w_{34}(F_{C341} + F_{K341} - F_{C342} - F_{K342}) - \mathrm{M}_{T3} - M_{T4} + M_{kx} \end{cases} \quad (8)$$

2.2. Motion Equation of the Axles

The axle is connected to the vehicle body through the suspension system. The Newton-Euler equation, expanded in the roll plane for three degrees of freedom according to the 3 equations of motion of the axle, can be written as follows.

$$\begin{cases} m_{ai}\dot{v}_{yai} - m_{ai}(\omega_{xai}v_{zai} - \omega_{zai}v_{xai}) = F_{AYi} \\ m_{ai}\dot{v}_{zai} - m_{ai}(\omega_{yai}v_{xAi} - \omega_{xai}v_{yai}) = F_{AZi} \\ I_{axi}\dot{\omega}_{xai} - (I_{yai} - I_{zai})\omega_{yai}\omega_{zai} = M_{AXi} \end{cases} \quad (9)$$

where: m_{ai} and I_{axi}, I_{ayi}, and I_{azi} are the mass and moment of inertia of the axle, respectively; F_{AYi} and F_{AZi} are the total external forces in the A_iy_{ai} and A_iz_{ai} directions of the axle, respectively; M_{Axi} is the total moment along the A_ix_{ai} axis.

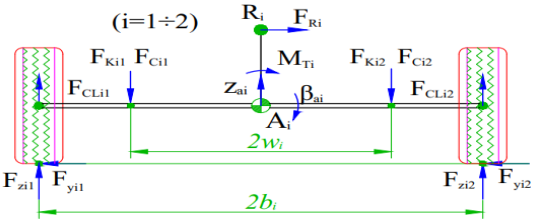

Fig. 2. Schematic dynamics of 1st axle and 2nd axle on the roll plane

Fig. 2 shows the external forces and moments acting on the first and second axles in the roll plane. These forces and moments can include lateral forces at the tires, leaf spring force F_{Cij}, damping force F_{Kij}, lateral force at the center of roll center F_{Ri}, and roll moment M_{Ti}. They can be expressed using the following formula as:

$$\begin{cases} F_{AYi} = F_{xi1}\sin\delta_{i1} + F_{yi1}\cos\delta_{i1} + F_{xi2}\sin\delta_{i2} + F_{yi2}\cos\delta_{i2} \\ \qquad - F_{Ri} - m_{ai}g\cos\varphi_i\sin\beta_{ai} \\ F_{AZi} = F_{CLi1} + F_{CLi2} - (F_{Ci1} + F_{Ci2} + F_{Ki1} + F_{Ki2}) \\ \qquad + m_{ai}g(1 - \cos\varphi_{ai}\cos\beta_{ai}) \\ M_{AXi} = (F_{CLi1} - F_{CLi2})b_i + (F_{Ci2} + F_{Ki2} - F_{Ci1} - F_{Ki1})w_i \\ \qquad + F_{Ri}(h_{Ri} - r_i) + (F_{xi1}\sin\delta_{i1} + F_{yi1}\cos\delta_{i1} \\ \qquad + F_{xi2}\sin\delta_{i2} + F_{yi2}\cos\delta_{i2})r_i + M_{Ti} \end{cases} \quad (10)$$

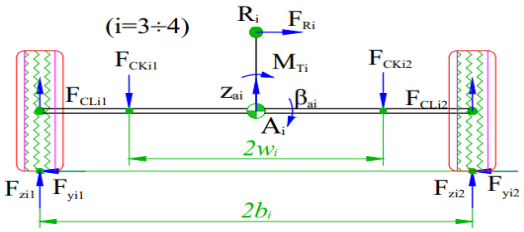

Fig. 3. Schematic dynamics of the 3rd axle and 4th axle on the roll plane

The "Walking Beam" suspension system connects the 3rd and 4th axles to the vehicle body. This results in vertical forces, known as F_{CKij} forces, acting

on the suspension system at points above and below it, as shown in Fig. 3. The total external forces acting on the 3rd and 4th axles in the roll plane can be calculated using the following formula as:

$$\begin{cases} F_{AYi} = F_{yi1} + F_{yi2} - F_{Ri}^{'} - m_{ai} g \cos\varphi_{ai} \sin\beta_{ai} \\ F_{AZi} = (F_{CLi1} + F_{CLi2}) - (F_{CKi1} + F_{CKi2}) \\ \qquad + m_{ai} g (1 - \cos\varphi_{ai} \cos\beta_{ai}) \\ M_{AXi} = (F_{CLi1} - F_{CLi2}) b_i + (F_{CKi2} - F_{CKi1}) w_i \\ \qquad + F_{Ri}(h_{Ri} - r_1) + (F_{yi1} + F_{yi2}) r_i + M_{Ti} \end{cases} \quad (11)$$

2.3. Dynamics of Wheels

To accurately describe the motion of a vehicle, it is crucial to determine the longitudinal and lateral forces acting on its wheels. This article will focus on the relative rotation between the wheel and the axle. The angular velocity of the wheel is used as an input parameter to calculate the longitudinal slip and lateral slip angles, which are then used in tire models to determine the forces at the tire-road interface. The general dynamic equations for 8 wheels are as follows:

$$I_{Wij}\dot{\omega}_{Wij} = T_{Wij} - F_{xij} r_{dij} \quad (i = 1 \div 4; j = 1 \div 2) \quad (12)$$

where ω_{Wij} are the angular velocities of the wheels; F_{xij} are the longitudinal forces; T_{Wij} are the moment applied to the wheels ij; I_{Wyij} are the moment of inertia of the wheels about the $W_{ij}y_{ij}$ axis; r_{dij} are the dynamic radius of the wheels.

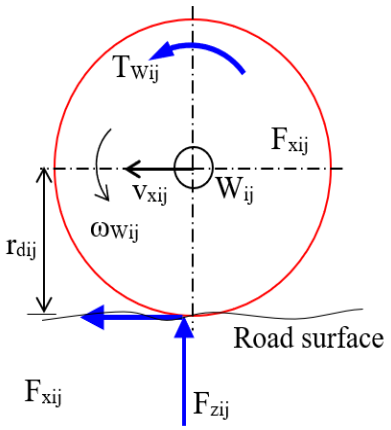

Fig. 4. Schematic dynamics of the wheels

3. Determined the Applied Forces and Moments

3.1. Burckhardt Tire Model

The tire force on each wheel consists of three components: longitudinal force (F_{xij}), lateral force (F_{yij}), and vertical force (F_{zij}). These forces are influenced by factors such as tire structure, road pavement,... To accurately model vehicle dynamics, a tire model is commonly used. In this study, the Burckhardt tire model is used, with coefficients C_1=0.857, C_2=33.82, and C_3 = 0.35 and a maximum adhesion coefficient of 0.8 [12]. The Burckhardt model is used to calculate the longitudinal and lateral forces at the wheel, as shown in equation system as follows:

$$\begin{cases} F_{xij} = \dfrac{s_{xij}}{\sqrt{s_{xij}^2 + s_{yij}^2}} (C_1 \left(1 - e^{-C_2\sqrt{s_{xij}^2 + s_{yij}^2}}\right) - C_3 \sqrt{s_{xij}^2 + s_{yij}^2}) F_{zij} \\ F_{yij} = \dfrac{s_{yij}}{\sqrt{s_{xij}^2 + s_{yij}^2}} (C_1 \left(1 - e^{-C_2\sqrt{s_{xij}^2 + s_{yij}^2}}\right) - C_3 \sqrt{s_{xij}^2 + s_{yij}^2}) F_{zij} \end{cases} \quad (13)$$

s_{xij} are the longitudinal slip coefficients on each wheel are calculated according to the following formula:

$$s_{xij} = \begin{cases} -\dfrac{v_{xij} - r_{dij}\omega_{Wij}}{v_{xij}} & \text{khi} \quad -1 \le s_{xij} \le 0 \\ \dfrac{r_{dij}\omega_{Wij} - v_{xij}}{r_{dij}\omega_{Wij}} & \text{khi} \quad 0 < s_{xij} < 1 \end{cases} \quad (14)$$

s_{yij} are the slip angles at the wheel depending on each wheel and they are calculated according to the following formula

$$s_{yij} = \delta_{ij} - atan\left(\frac{v_{yai}}{v_{xai} + (-1)^{j-1} b_i \omega_z}\right) \quad (15)$$

F_{zij} are the total vertical forces on each wheel are calculated according to the following formula:

$$\begin{cases} F_{zij} = F_{CLij} + F_{zstij} \\ F_{CLij} = \begin{cases} C_{Lij}\left(h_{ij} - z_{Aij}\right) & when \quad wheel \quad is \quad "lift-on" \\ -F_{zstij} & when \quad wheel \quad is \quad "lift-off" \end{cases} \end{cases} \quad (16)$$

3.2. Suspension Model

The suspension systems for the 1st and 2nd axles utilize solid suspension systems, which consist of leaf springs and hydraulic dampers. The spring and damper forces can be calculated using the following equations:

$$\begin{cases} F_{Cij} = \begin{cases} C_\infty\left(z_{aij} - z_{sij} + f_{dij}^n\right) & when \quad f_{dij}^n < z_{aij} - z_{sij} \\ C_{ij}\left(z_{aij} - z_{sij}\right) & when \quad f_{dij}^t \le z_{aij} - z_{sij} \le f_{dij}^n \\ -C_\infty\left(z_{aij} - z_{sij} - f_{dij}^n\right) & when \quad z_{aij} - z_{sij} < f_{dij}^n \end{cases} \\ F_{Kij} = K_{ij}\left(\dot{z}_{aij} - \dot{z}_{sij}\right) \end{cases} \quad (17)$$

The vertical motion of the upper and lower link points of the 1st and 2nd axle suspension system is determined by the vertical motion of the CoG of the vehicle body in the body coordinate system, as well as the pitch angle φ and roll angle β_1. We calculate the vertical motion of the lower link points of the 1st and 2nd axle suspension system from the motion of the CoG of axle z_{ai} and the roll angle β_{ai} as:

$$\begin{cases} z_{sij} = z - l_i \sin\varphi + (-1)^{j-1} w_i \sin\beta_1 \\ z_{aij} = z_{ai} + (-1)^{j-1} w_i \sin\beta_{ai} \end{cases} \quad (18)$$

To calculate the distribution of the suspension force in the "Walking Beam" suspension system, it is necessary to describe two rigid beams that join the 3rd and 4th axles. These beams A_1A_2 and B_1B_2 have a moment of inertia for left and right I_{ayL}, and I_{ayR}, respectively as:

$$\begin{cases} I_{ayL}\ddot{\varphi}_L = -F_{CK31}\dfrac{a}{2} + F_{CK41}\dfrac{a}{2} \\ I_{ayR}\ddot{\varphi}_R = -F_{CK32}\dfrac{a}{2} + F_{CK42}\dfrac{a}{2} \end{cases} \quad (19)$$

The spring forces and the damper forces of the "Walking Beam" suspension system can be calculated as follows:

$$\begin{cases} F_{C34j} = \begin{cases} C_\infty\left(z_{a34j} - z_{S34j} + f^n_{d34j}\right) & when \quad f^n_{d34j} < z_{a34j} - z_{S34j} \\ C_{34j}\left(z_{a34j} - z_{S34j}\right) & when \quad f^t_{d34j} \le z_{a34j} - z_{S34j} \le f^n_{d34j} \\ -C_\infty\left(z_{a34j} - z_{S34j} - f^n_{d34j}\right) & when \quad z_{a34j} - z_{a34j} < f^n_{d34j} \end{cases} \\ F_{K34j} = K_{34j}\left(\dot{z}_{a34j} - \dot{z}_{a34j}\right) \end{cases} \quad (20)$$

The motions of these beams are vertical motion and pitch angle z_{a341}, z_{a342} respectively. The vertical motion of the above and lower of the "Walking Beam" suspension system can be determined as follows:

$$\begin{cases} z_{s341} = z + \dfrac{l_3 + l_4}{2}\sin\varphi + \dfrac{w_3 + w_4}{2}\sin\beta_2 \\ z_{s342} = z + \dfrac{l_3 + l_4}{2}\sin\varphi - \dfrac{w_3 + w_4}{2}\sin\beta_2 \\ z_{a341} = \dfrac{1}{2}(z_{a3} + z_{a4} + w_3\sin\beta_{a3} + w_4\sin\beta_{a4}) \\ z_{a342} = \dfrac{1}{2}(z_{a3} + z_{a4} - w_3\sin\beta_{a3} - w_4\sin\beta_{a4}) \end{cases} \quad (21)$$

Roll angles of the axles are calculated as:

$$\beta_{ai} = \int\left(\omega_{xai} + \omega_y\sin\beta_{ai}\tan\varphi + \omega_z\tan\varphi\cos\beta_{ai}\right)dt \quad (22)$$

The moments due to frame torsion and roll moment are calculated as follows:

$$\begin{cases} M_{kx} = C_{kx}(\beta_2 - \beta_1) \\ M_{T1} = C_{T1}(\beta_{a1} - \beta_1) \\ M_{T2} = C_{T2}(\beta_{a2} - \beta_1) \\ M_{T3} = C_{T3}(\beta_{a3} - \beta_2) \\ M_{T4} = C_{T4}(\beta_{a4} - \beta_2) \end{cases} \quad (23)$$

3.3. Model of 2-Axle Steering System

When the driver acts on the steering wheel, the wheels will turn at corresponding angles to make the vehicle turn. With 2 axles steer on the front, the steer wheels are linked via levers to ensure correct kinematics when turning [7]. The wheels on a steering axle still ensure alignment and are described by the Ackermann formula with the steering wheel rotation angle δ_{SW} being the input rule according to the following formulas:

$$\begin{cases} \delta_{11} = \dfrac{1}{i_S}\delta_{SW}(t) \\ \delta_{12} = a\tan\dfrac{\tan\delta_{11}}{1 + \dfrac{2b_1\tan\delta_{11}}{l_1 + l_3 + 0.5a}} \\ \delta_{21} = a\tan\left[\dfrac{l_2 + l_3 + 0.5a}{l_1 + l_3 + 0.5a}\tan\delta_{11}\right] \\ \delta_{22} = a\tan\dfrac{\tan\delta_{21}}{1 + \dfrac{2b_2\tan\delta_{21}}{l_2 + l_3 + 0.5a}} \end{cases} \quad (24)$$

4. Assessment Parameters

After solving the system of 30 equations including 6 equations of the system of equations (1), 2 equations of the system of equations (2), 12 equations of the system of equations (9), and 8 equations of the system of equations (12). Some motion assessment parameters can be calculated. Lateral acceleration and roll angle of the vehicle body are calculated as:

$$\begin{cases} a_y = \dot{v}_y + \omega_z v_x - \omega_x v_z \\ \beta = \int\left(\omega_x + \omega_y\sin\beta\tan\varphi + \omega_z\cos\beta\tan\varphi\right)dt \end{cases} \quad (25)$$

The LTR on each axle (LTR_i) is a measure used to determine the wheel separation state of an axle [6-8]. Lift-off is the phenomenon in which one side of the wheel on an axle separates from the road surface. When liff-off occurs on an axle, the LTR on that axle is equal to 1. The calculation formula for 4 vehicle axles is as follows:

$$LTR_i = \frac{F_{zi2} - F_{zi1}}{F_{zi2} + F_{zi1}} \ (i = 1 \div 4) \quad (26)$$

The LTR is a measure of the load distribution of the whole vehicle [6 - 8]. For a 4-axle truck vehicle, the formula is as follows.

$$LTR = \frac{\sum_{i=1}^{4}(F_{zi2} - F_{zi1})}{\sum_{i=1}^{4}(F_{zi2} + F_{zi1})} \quad (27)$$

5. Results and Discussions

The dynamics model is simulated by MATLAB-Simulink software with the parameters of the vehicle labeled HOWO 8×4 HW76 380HP [13], as shown in the table below.

Table 1. The structure parameters of a 4-axle truck vehicle.

Parameters (Symbol)	**Values (Unit)**
Mass of vehicle body (m)	26400 (kg)
Mass of the first and second axles (m_{a1},m_{a2})	570 (kg)
Mass of the third and fourth axles (m_{a3},m_{a4})	785 (kg)
Roll moment of the inertia of front and rear mass (I_{x1}; I_{x2})	12810;17191.9 (kgm^2)
Roll moment of inertia the vehicle body (I_x)	30001.9(kgm^2)
Pitch moment of inertia the vehicle body (I_y)	203270.3 (kgm^2)
Yaw moment of inertia the vehicle body (I_z)	200768.5 (kgm^2)
Pitch moment of inertia of the rigid beam (I_{AyL}, I_{AyR})	600 (kgm^2)
Suspension stiffness of the suspension of the 1st and 2nd axles (C_{1j}, C_{2j})	250 (kN/m)
Suspension stiffness of the 3rd axle and 4th axle (C_{34j})	1400 (kN/m)
Damper coefficient of the suspension of the 1st axle and the 2nd axle (K_{1j}, K_{2j})	15000 (Ns/m)
Damper coefficient of the 3rd axle and 4th axle (K_{34j})	30000 (Ns/m)
Torsion coefficient of frame body (C_{kx})	4000 (kNm/rad)
Torsion coefficient of stabilizing bar of the 1st axle and the 2nd axle (C_{T1}, C_{T2})	28.648 (kNm/rad)
Torsion coefficient of stabilizing bar of the 3rd axle and 4th axle (C_{T3}, C_{T4})	171.890 (kNm/rad)
Vertical stiffness of the tire of the 1st axle and the 2nd axle (C_{L1j}, C_{L2j})	980 (kN/m)
Vertical stiffness of the tire of the 3rd axle and 4th axle (C_{L3j}, C_{L4j})	1960 (kN/m)
Distance from CoG to the axle i (l_i)	3.674;1.874; 1.326; 2.676 (m)
Height of vehicle body's CoG (h)	1.700 (m)
Half-track width of the axles (b_i)	1.0205;1.0205; 0.925;0.925 (m)
Half spring spacing of the axles (w_i)	0.6;0.6;0.5;0.5 (m)
Diameter of tire (r)	0.512 (m)

A survey was conducted on the performance with a steering wheel angle of 175 degrees, as shown in Fig. 5. The Magnitude of Steering Wheel Angle (MSWA) was used in the simulation for initial speeds (v_{int}) ranging from 5km/h to 65km/h. The road steer angle was calculated from the steering wheel angle with the ratio i_{SW}=1/25, as shown in formula (24) and presented in Fig. 6. As the vehicle's speed increased, its response changed accordingly. At speeds of 60 or 65km/h, the vehicle became unstable and prone to rollover. This was shown in the roll angle of the vehicle body, which reached 51.5 degrees at a speed of 65km/h after 3.8 sec of the survey.

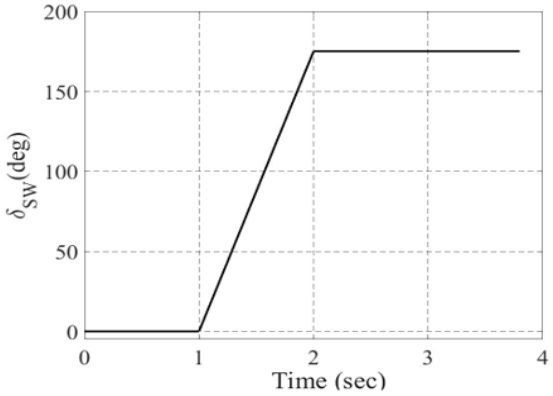

Fig. 5. Steering wheel angle.

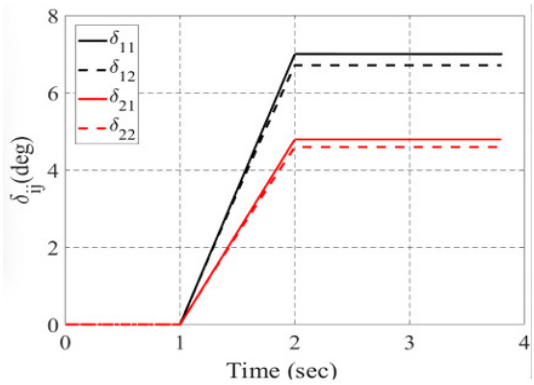

Fig. 6. Road steer angle.

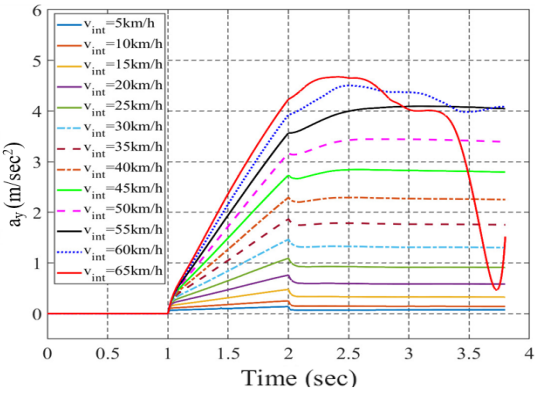

Fig. 7. Lateral acceleration of vehicle body.

The results of the survey showed that at a speed of 60 km/h, the vehicle was in a rollover condition, with a maximum lateral acceleration of 4.503m/sec^2 at

2.505 sec in the survey. This was earlier than the time of 3.44 sec when LTR and LTR_1 reached 1, but later than the time of 2.284 sec when LTR_4 reached 1. This indicates that the LTR_i coefficients at the axles can be used to predict the onset of rollover. The survey also determined that the 4th axle experienced early lift-off, followed by the front axle.

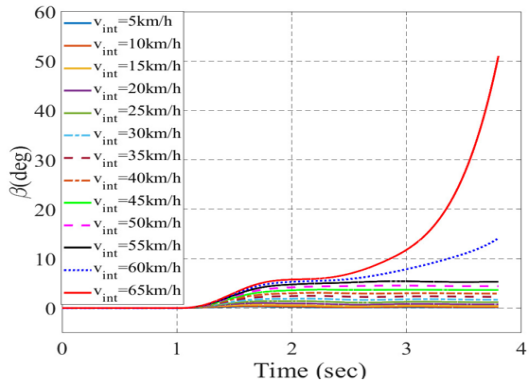

Fig. 8. Roll angle of the vehicle body

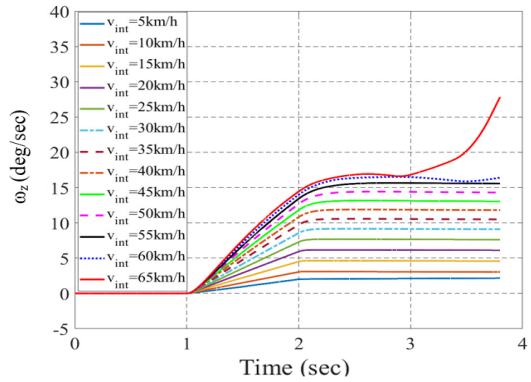

Fig. 9. Yaw rate of the vehicle body

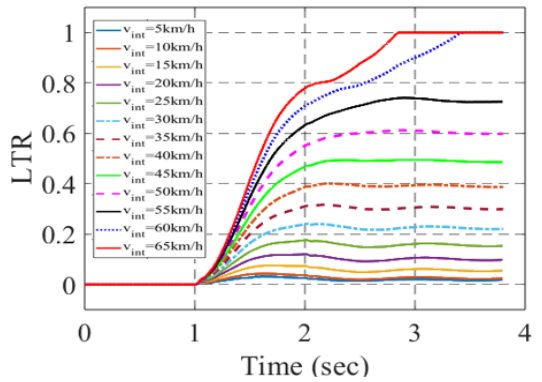

Fig. 10. Load Transfer Ratio of the whole vehicle

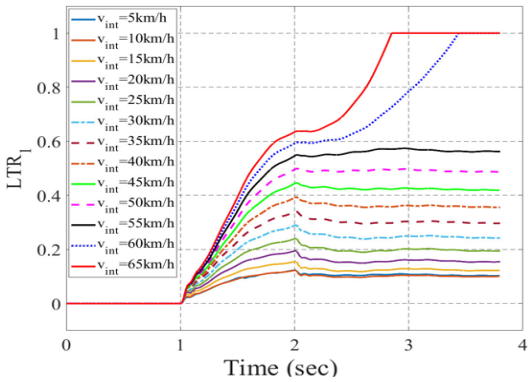

Fig. 11. Load Transfer Ratio of the 1st axle

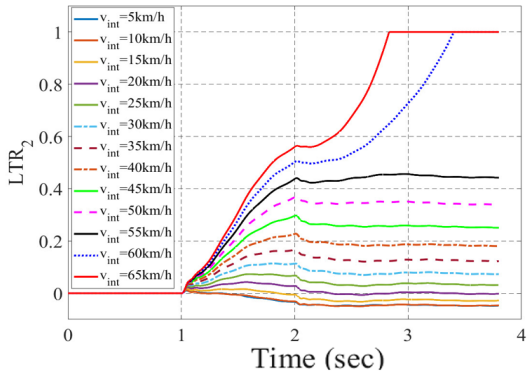

Fig. 12. Load Transfer Ratio of the 2nd axle

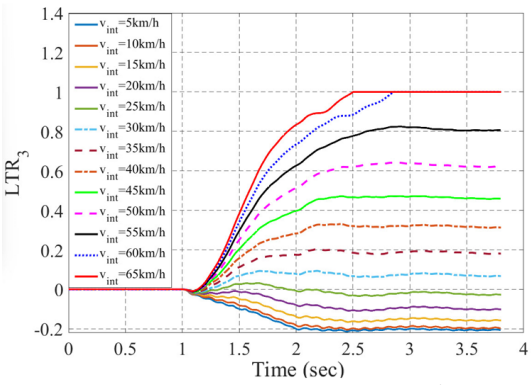

Fig. 13. Load Transfer Ratio of the 3rd axle

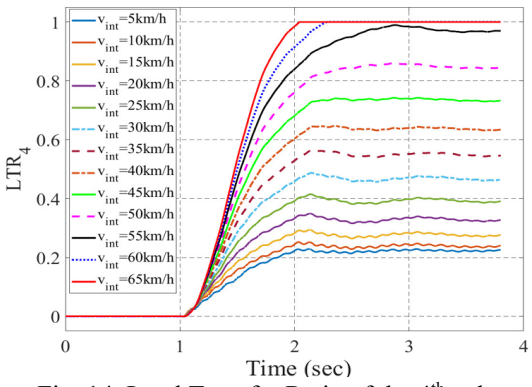

Fig. 14. Load Transfer Ratio of the 4th axle

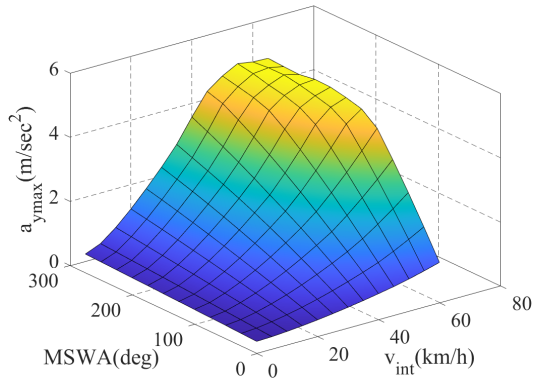

Fig. 15. Max of lateral acceleration of vehicle body

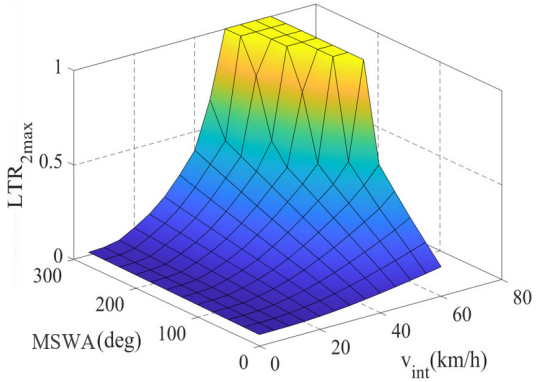

Fig. 19. Max of LTR_2

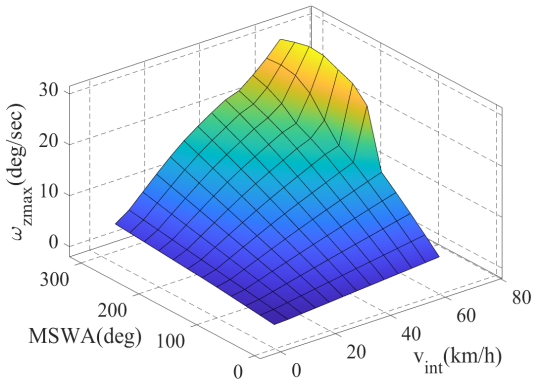

Fig. 16. Max of yaw rate of the vehicle body

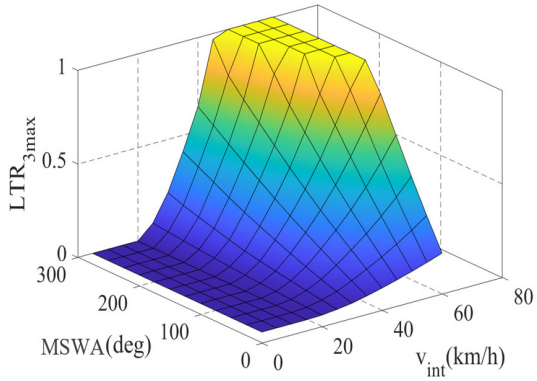

Fig. 20. Max of LTR_3

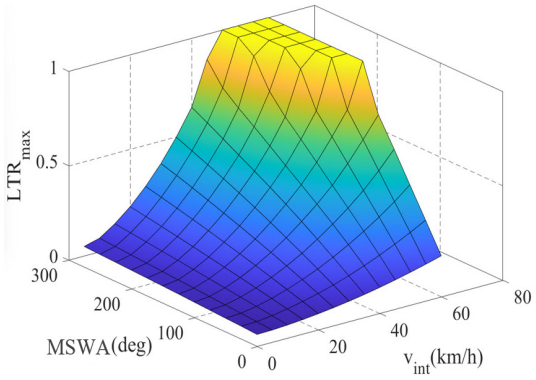

Fig. 17. Max of LTR

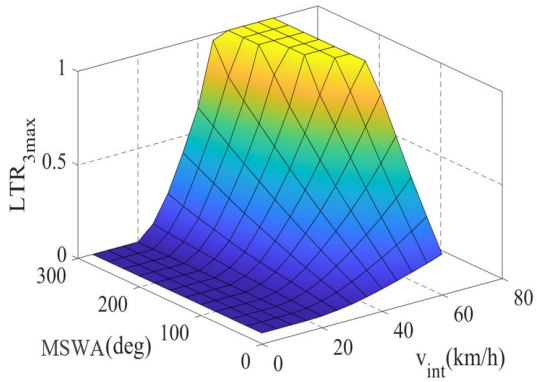

Fig. 21. Max of LTR_4

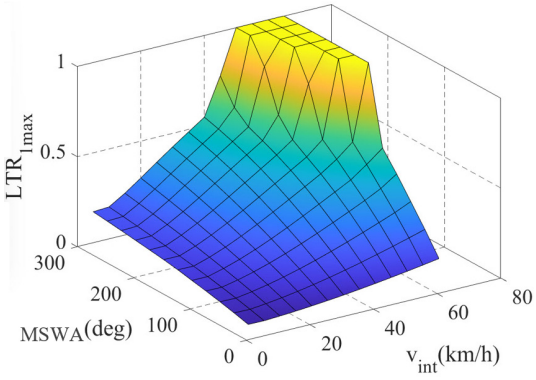

Fig. 18. Max of LTR_1

The survey was conducted with a range of MSWA from 25 degrees to 300 degrees and initial speeds ranging from 5 to 56 km/h. Fig. 15 shows the maximum lateral acceleration of the vehicle body at different speeds and MSWA ranges. Fig. 17 to Fig. 21 illustrate the maximum *LTR* and LTR_i values at different speeds and MSWA ranges. These results demonstrate the combined influence of vehicle speed and steering wheel angle on the rollover condition of the 4-axle truck vehicle. Rollover can be determined from Fig. 17, where *LTR* values equal 1. Furthermore, the region where LTR_i equals 1 on the independent vehicle axles (Fig. 18 to Fig. 21) can also indicate an early warning of a potential rollover condition. The results of this article can serve as a foundation for

designing active control systems to improve the motion stability of 4-axle truck vehicles.

6. Conclusion

Rollover is the main cause of accidents involving multi-axle truck vehicles. The article presents the results of a study on the rollover of a 4-axle truck vehicle using a 30-DOFs dynamic model. The model describes the vehicle body with 6 DOFs representing the movements of the center of gravity and 2 DOFs representing the roll angle of the front and rear mass of the vehicle. The Burckhardt tire model was utilized to calculate the tire force. The study surveyed 4-axle truck vehicle turning at initial speeds ranging from 5 to 65 km/h and at MSWA ranging from 25 to 300 degrees. The results demonstrate the complexity of the vehicle response. The article determined the range of parameters for the steering wheel angle and vehicle speed at which the vehicle is at risk of rollover (*LTR* is equal to 1). This model can be used to analyze the dynamics of 4-axle truck vehicle and their combined effects, providing a basis for developing warning and control systems for multi-axle truck vehicles.

References

[1] Fatality Facts 2022 Large trucks, Insurance Institute for Highway Safety, VA, USA, 2022. [Online]. Available: https://www.iihs.org/topics/fatality-statistics/detail/large-trucks

[2] M. Chen, L. Zhou, S. Choo and H. Lee, Analysis of risk factors affecting urban truck traffic accident severity in Korea, Sustainability, vol. 14, iss. 5, Mar. 2022. https://doi.org/10.3390/su14052901

[3] A. E. Mustafa, T. E. Mümin and O. Basar, Lateral Stability Control of articulated heavy vehicles based on active steering system, International Journal of Mechanical Engineering and Robotics Research, vol. 11, no. 8, pp. 575-582, Aug. 2022. https://doi.org/10.18178/ijmerr.11.8.575-582

[4] Y. Yanna, W. Huiying, S. Lu and H. Wei, Study on the influence of road geometry on vehicle lateral instability, Journal of Advanced Transportation, vol. 2020, iss.1, pp. 1- 15, Oct. 2020. https://doi.org/10.1155/2020/7943739

[5] T. T. Hung, V. V. Huong and D. N. Khanh, Study on the dynamic rollover indicators of tractor semi-trailer vehicle while turning maneuvers based on Multibody System Dynamics analysis and Newton-Euler equations, in Proc. AMAS 2021, Ha Long City, Vietnam, May. 2022, pp. 30-38. https://doi.org/10.1007/978-3-030-99666-6_5

[6] Z. Ye, W. Xie, Y. Yin and Z. Fu, Dynamic rollover prediction of heavy vehicles considering critical frequency, Automotive Innovation, vol. 3, pp. 158-168, Jun. 2020. https://doi.org/10.1007/s42154-020-00099-w

[7] M. M. Topaç, O. Çolak, L. Bilal, A. Tanriverdi, M. Karaka and M. Maviş, Structural analysis of a multi-axle steering linkage for an 8 × 8 special purpose vehicle, in Proc. VAE, Miskolc, Hungary, 2020, pp. 67-78. https://doi.org/10.1007/978-981-15-9529-5_6

[8] K. Lundahl, C. Lee, E. Frisk and L. Nielsen, Analyzing rollover indices for critical truck maneuvers, SAE International Journal of Commerical Vehicles, vol. 8, iss. 1, pp. 189-196, 2015. https://doi.org/10.4271/2015-01-1595

[9] L. Q. Jin and X. S. Chuan, A parameterized simulation model for multi-axle vehicle, Advanced Materials Research, Trans Tech Publications, Ltd., Jan. vol. 186, 2011, pp. 170-175. https://doi.org/10.4028/www.scientific.net/amr.186.170

[10] R. Piłatowicz and W. Luty, Modelling of dynamics of the suspension of tandem axles of a multi-axle vehicle provided with a novel load-equalising system, IOP Conf. Series: Materials Science and Engineering, vol. 1247, 2022. https://doi.org/10.1088/1757-899X/1247/1/012019

[11] Y. Chen, F. You, X. Li and L. Fu, Research and optimization of vehicle handling stability based on multi - body dynamics, IOP Conf. Series: Materials Science and Engineering, vol. 688, iss.3, 2019.

https://doi.org/10.1088/1757-899X/688/3/033009

[12] H. Guan, B. Wang, P. Lu and L. Xu, Identification of maximum road friction coefficient and optimal slip ratio based on road type recognition. Chinese Journal of Mechanical Engineering,vol. 27, pp. 1018-1026, Aug. 2014. https://doi.org/10.3901/CJME.2014.0725.128

[13] 12 Wheels Euro 2 HW76 Cabin Sinotruk Howo 8x4 Dump Truck-howo, SINOTRUK HOWO. [Online]. Available: https://sinotrukhowo.cn/portfolio-item/howo-howo-9/